J. Membrane Biol. 180, 33–48 (2001)
DOI: 10.1007/s002320010057

The Journal of
Membrane
Biology

Formation of Flat Lamellar Intramembrane Lipid Structures in Microorganisms

V.I. Duda[1], N.E. Suzina[1], L.O. Severina[2], V.V. Dmitriev[1], G.I. Karavaiko[2]

[1]Skryabin Institute of Biochemistry and Physiology of Microorganisms, Russian Academy of Sciences, pr. Nauki 5, Pushchino, Moscow Region, 142290 Russia

[2]Institute of Microbiology, Russian Academy of Sciences, pr. 60-letiya Oktyabrya 7, k. 2, Moscow, 117811 Russia

Received: 17 July 2000/Revised: 22 November 2000

Abstract. Analysis of freeze-fracture replicas and thin sections of cells of the bacteria *Sulfobacillus thermosulfidooxidans* and *Anaerobacter polyendosporus* showed that their cytoplasmic membranes contain some regions in the form of flat lamellar inverted lipid membranes a few tenths of nanometers to a few microns in size. The specific features of these membrane structures are as follows: (i) they contain no familiar intramembrane particles commonly present on freeze-fracture replicas; (ii) in cross thin sections, intramembrane structures are bifurcate on the periphery and look like thylakoids; and (iii) the leaflets of intramembrane structures in *S. thermosulfidooxidans* cells are corrugated. These structures were revealed in bacterial cells cultivated under normal growth conditions. The data obtained suggest the occurrence of a complex type of compartmentalization in biological membranes.

Key words: Microbial membranes — Intramembrane structures — Inverted lipid membranes — Cell ultrastructure

Introduction

The modern concept of the structure of biomembranes is based on the idea of a lipid bilayer as the main structural unit of eukaryotic and prokaryotic membranes. However, the cytoplasmic membrane of some archaea is made up of a single layer of specific bipolar lipids (Langworthy, Tornabene & Holzer, 1982; Gliozzi et al., 1982; Rolandi et al., 1986). Moreover, there have been reports indicating that lipid molecules may form nonbilayer structures in some regions of membranes, such as hexagonal HI and HII phases, cubic and rhombic particles, and inverted lipid micelles and vesicles (Cullis et al., 1980; Borovjagin, Vargara & McIntosh, 1982; Verkleij, 1984; Borovjagin et al., 1987; Borovjagin & Sabelnikov, 1989; Epand, 1998; May & Ben-Shaul, 1999). It should, however, be noted that most of these observations were made in experiments with artificial membranes, whereas little is known about the formation of nonbilayer lipid structures in natural biomembranes.

Gram-positive bacteria are a convenient model for studying the structure of biomembranes, since they have only the cytoplasmic membrane, which considerably simplifies the interpretation of photomicrographs. When studying the ultrastructure of cells of novel bacterial species, *Anaerobacter polyendosporus* (Siunov et al., 1999) and *Sulfobacillus thermosulfidooxidans* (Suzina, 1999), we found that some regions of their cytoplasmic membranes (CMs) contain multilayer structures.

In this work, we present evidence that these structures can be considered as flat lamellar intramembrane structures (LIMS).

Materials and Methods

Bacterial Strains

In this study we used two gram-positive bacteria, which do not possess outer cell membrane and distinct intracytoplasmic membranes. *Sulfobacillus thermosulfidooxidans* strain VKM B-1269 (= DSM 9293) is a gram-positive aerobic thermoacidophilic spore-forming bacterium capable of oxidizing sulfur, its reduced compounds, sulfide minerals, and ferrous oxide at low pH values (1.0–3.5) in a temperature range of 30 to 58°C (Golovacheva & Karavaiko, 1978). This bacterium is a member of the *Clostridium–Bacillus* subphylum and forms one phylogenetic cluster with the genus *Alicyclobacillus* (Tourova et al., 1994). *Anaerobacter polyendosporus* strain PS-1 is an obligately anaerobic mesophilic heterotrophic bacterium capable of forming 6–7 endospores per

Correspondence to: V.I. Duda

cell. In physiology and phylogeny, this bacterium is close to saccharolytic species of the genus *Clostridium* (Siunov et al., 1999).

Growth Media and Cultivation Conditions

S. thermosulfidooxidans strain VKM B-1269 was grown in five media. Medium 1 contained (g/l distilled water) (NH4)2SO4, 6.0; K2HPO4, 0.2; KCl, 0.2; MgSO4 · 7H2O, 1.0; Ca(NO3)2, 0.02; and yeast extract, 0.2 (pH 2.25). Media 2–5 were as medium 1 except that they were additionally supplemented with 0.5 g/l glucose, 2.5 g/l pyrite, 33.4 g/l FeSO4 · 7H2O, and 0.5 g/l elemental sulfur, respectively. The pH of these media was 2.25. The cultivation time was 1–5 days. *S. thermosulfidooxidans* was cultivated in shaken (160 rpm) 250-ml Erlenmeyer flasks containing 100 ml of the growth medium. To maintain the bacterium in the active state, it was alternatively grown either in medium 3 or in medium 4 to change the mineral source of energy (ferrous oxide or pyrite) (Tsaplina et al., 1991). Growth was monitored by measuring the protein content of the culture (Hartree, 1972). Cells for the preparation of specimens were separated from the culture liquid by centrifugation at 4,500 × *g* for 30 min and washed with medium 1 from which yeast extract was omitted.

An. polyendosporus strain PS-1 was grown anaerobically at 28°C on potato agar (PA) or in a synthetic medium with glucose as the carbon and energy source (Duda et al., 1987).

Thin Sectioning

Bacterial cells were prefixed with a 1.5% solution of glutaraldehyde in 0.05 M cacodylate buffer (pH 7.2) at 4°C for 1 hr. After thrice washing with this buffer, the material was refixed with 1% solution of OsO4 in the same buffer at 20°C for 3 hr and dehydrated. The material was then embedded in Spurr epoxy resin and cut into thin sections. The sections were mounted on Formvar-coated grids and contrasted with a 3% solution of uranyl acetate in 70% ethanol and then with lead citrate (Reynolds, 1963) at 20°C for 4–5 min. Freeze-substitution thin sections were prepared as described by Hoch (1986). Cells were rapidly fixed with liquid propane (−196°C) and dehydrated in a temperature-controlled chamber with cold acetone (−85°C) containing 1% OsO4. After dehydration, the material was embedded in Spurr epoxy resin and cut into thin sections, which were then mounted on grids and further contrasted with lead citrate (Reynolds, 1963).

Freeze-Fracturing

We carried out freeze-fracturing in a JEE-4X vacuum evaporator equipped with an accessory providing a rapid quenching of microbial cells at a rate of about 106°C/s (Fikhte, Zaichkin & Ratner, 1973). The preliminary steps of biomass preparation for cryofixation (centrifugation of cells and their transfer to the evaporator) were carried out either at room temperature (20°C) or cultivation temperature (28 and 48°C for *An. polyendosporus* and *S. thermosulfidooxidans,* respectively). In some experiments, cells were fixed with a 1.5% solution of glutaraldehyde in 0.06 M cacodylate buffer (pH 7.2) at 4 or 48°C for 1 hr. The material was placed in liquid propane overcooled to −196°C with liquid nitrogen and freeze-fractured at −100°C at a pressure of 3×10^{-4} Pa. Replicas of freeze-fractured cells were prepared by shadowing with a platinum–carbon mixture at an angle of 30° and then of carbon alone at an angle of 90°.

Results

The analysis of the freeze-fracture replicas and thin sections of *S. thermosulfidooxidans* cells allowed us to reveal the following ultrastructural features of this bacterium. Like other bacteria, *S. thermosulfidooxidans* exhibited the presence of EF face and PF face (the latter with a great number of IMPs about 10 nm in diameter) in freeze-fracture replicas. However, the CM of this bacterium also contained numerous randomly distributed narrow pocketlike invaginations (PLIs) 0.05 to 0.4 μm long (Figs. 1, 4 and 7). PLIs were observed on both faces of the CM and contained no IMPs. The number, orientation, and the length of PLIs in *S. thermosulfidooxidans* cells did not depend on the cultivation media in which they were grown, except the cells grown in medium 3 with pyrite, which were found to have invaginations as long as a whole bacterial cell (up to 1 μm in length) predominantly located near growing septa. The surface density of PLIs on freeze-fracture replicas strongly depended on cultivation temperature and the temperatures at which the biomass was prepared for cryofixation. When the cultivation temperature was changed from 28°C to 48–50°C, the number of the PLIs observed per μm^2 of freeze-fracture replica varied from 2–5 to 0–3. However, as the temperature at which the biomass was prepared for cryofixation was changed from 48–50 to 20°C, the surface density of PLIs increased to 50–60 per μm^2. The results were essentially the same if, before cryofixation, cells were prefixed with 1.5% glutaraldehyde. It should be noted that we were the first to observe PLIs in the CM of prokaryotic cells, although such structures had already been observed in yeast cells, which, unlike bacterial cells, additionally contain IMPs (Moore & Muhletaler, 1963).

In freeze-fractured replicas, the LIMSs of sulfobacilli looked like sheets of different forms and sizes (Figs. 1–9) sometimes covering up to half the visible surface of the replica of a longitudinally fractured cell. These smooth IMP-lacking sheets of LIMSs were found to overlie the PF or EF face of the CM. The sheet edges are abrupt, so that shadowing the replicas led to the deposition of Pt on the edges. As for conventional prominences and depressions on the PF and EF faces, they look smooth and without abrupt edges.

Analysis showed that up to 60% of young cells contain such structures (*see* Table) irrespective of the cultivation medium and temperature (48–50°C or 28°C). In some cultures grown in medium 5 with elemental sulfur, the percentage of LIMS-containing cells increased to 80%. Inasmuch as the cytoplasmic membrane is fractured along the hydrophobic interior of the lipid bilayer and the LIMS leaflets in the electron micrographs of freeze-fracture replicas overlie the PF or EF face of the CM (Figs. 1–9), it can be inferred that LIMSs are located in the hydrophobic interior of the CM between its outer and inner leaflets. It can be seen from Figs. 1 and 9 that PLIs occur in part on the open PF face of the freeze-fracture replica and in part beneath the patchlike layer, as

Table Percentage of cells with LIMS of the total examined

Bacteria	Freeze-fracturing	Thin sectioning
Sulfobacillus thermosulfidooxidans, str. DSM 9293	30–60[1], 80[2]	10–20[2]
Anaerobacter polyendosporus PS-1	20–30[3] 60–80[4]	

[1] Cells were grown in medium 2 or 3.
[2] Cells were grown in sulfur-containing medium 5.
[3] Cells were grown on PA.
[4] Cells were grown anaerobically and then exposed to the air for 24 hr.

indicated by arrows in these figures. Hypothetically, intramembrane leaflets composed of nonpolar lipids can give similar images. In this case, however, these hydrophobic electron-transparent regions would be about 20–30 Å thicker in cross thin sections, which is not the case (*see below*).

In some cells, LIMSs have a distinct corrugated appearance (Figs. 4 and 8) because LIMS leaflets contain parallel ridges with a hemispherical profile spaced 32.4 nm apart. In different cells, the ridge thickness varies from about 20 to 27 nm, the interridge valley being 5.4 to 10.4 nm wide. In some cells, ridges longer than 0.5 μm are bent in their central part at an angle of 120 or 60° (*see* Fig. 8).

Figures 3 and 5 show the likely directions of fracture planes and Fig. 32*A–C*, the possible disposition of lipid molecules in membranes. Corrugated LIMSs can be observed in some spores situated in the cytoplasm (Fig. 9).

LIMS leaflets show either smooth (Fig. 4), granular, or curved appearance (Fig. 5). Some LIMSs have the alternating regions of regularly arranged ridges, smooth zones, and hemispheres with a diameter of about 250 Å (Fig. 7). The LIMSs described were observed in cells grown either organotrophically in the glucose-containing medium 2 or mixotrophically in medium 3 or 5 containing pyrite and elemental sulfur, respectively. The incidence, size and structural organization of intramembrane sheets depended on the growth phase of cells. The maximum number of such structures was observed in actively growing young cells from the early logarithmic growth phase (*see* Table). At the same time, the structural organization of LIMSs depended neither on the cultivation conditions (the composition of the growth medium and cultivation temperature) nor on the conditions of the preliminary steps of biomass preparation for cryofixation (the temperature of biomass preparation and the involvement of the glutaraldehyde fixation step).

As is evident from the electron micrographs of thin sections of cells prepared by the conventional methods of fixation and embedding (Figs. 10–21), the CM of *S. thermosulfidooxidans* cells has a trilaminar asymmetric profile with the electron-dense outer layer, which is thicker than the inner, cytoplasm-adjacent, layer. The CM of sulfobacilli is characterized by a pronounced bending and the presence of pocketlike invaginations directed toward the cytoplasm (Figs. 11 and 14). From outside, the CM is bounded by the cell wall (CW) usually composed of a single 25- to 30-nm-thick layer, which is typical of gram-positive bacteria. Some cells exhibited the presence of the surface S layer (Fig. 21), which was described in detail elsewhere (Severina et al., 1998). The cytoplasm contained electron-dense polyphosphate granules but no poly-β-hydroxybutyrate granules. In thin sections, the nucleoid looked like an electron-transparent slightly fibrillar zone. Thin sections also exhibited the presence of rare intracytoplasmic membrane structures of vesicular and looplike (tubular or helical) form (Fig. 10) and specific lamellar membrane structures (LIMSs) incorporated into the CM (Figs. 10–21). In the images that were made under low magnification, LIMS look like local thickenings of the CM (Fig. 10). But in the electron micrographs that were obtained under high magnification, the thin structure of LIMS can be seen (Figs. 11, 12, 14, 17, 19, 21).

Figures 13, 15, 16, 18, 20 give a schematic interpretation of the respective electron microscopic images. Some of the leaflets of multilamellar membrane structures occurred in the periplasmic space, and some were partially immersed in the cytoplasm. A unit LIMS was composed of three electron-dense layers interspaced by two electron-transparent layers representing hydrophobic lipid zones (Fig. 11–15). The central electron-dense layer with a thickness of about 60 Å was two times as thick as the peripheral electron-dense layers, which suggests that the central layer may represent two closely adjacent outer electron-dense membrane layers. On the periphery of LIMSs, the CM had a bifurcate profile, suggesting its cleavage along the hydrophobic region into two layers embracing the inner electron-dense (hydrophilic) and outer electron-transparent (hydrophobic) zones. These intramembrane structures exhibited the features that are typical of inverted lipid membranes. Cells may contain from one to several unit LIMS located either laterally or at the cell poles (Figs. 17–21).

Thin sections of cells prepared by the freeze-substitution method also exhibited the presence of LIMSs (Fig. 21). Although the CM images in this case had lower contrast than the images obtained by conventional methods (this was probably due to the fact that fixation and dehydration in cold acetone (−85°C) caused an insignificant loss of cellular components), alternating electron-transparent and electron-opaque layers and the bifurcate profile of the CM located on the LIMS periphery can be easily seen in these images.

Analysis of electron micrographs showed that at least some LIMSs were due to invaginations of the outer leaflet of the CM into the periplasmic space. As can be seen from Figs. 14 and 19 (such images are not rare), the

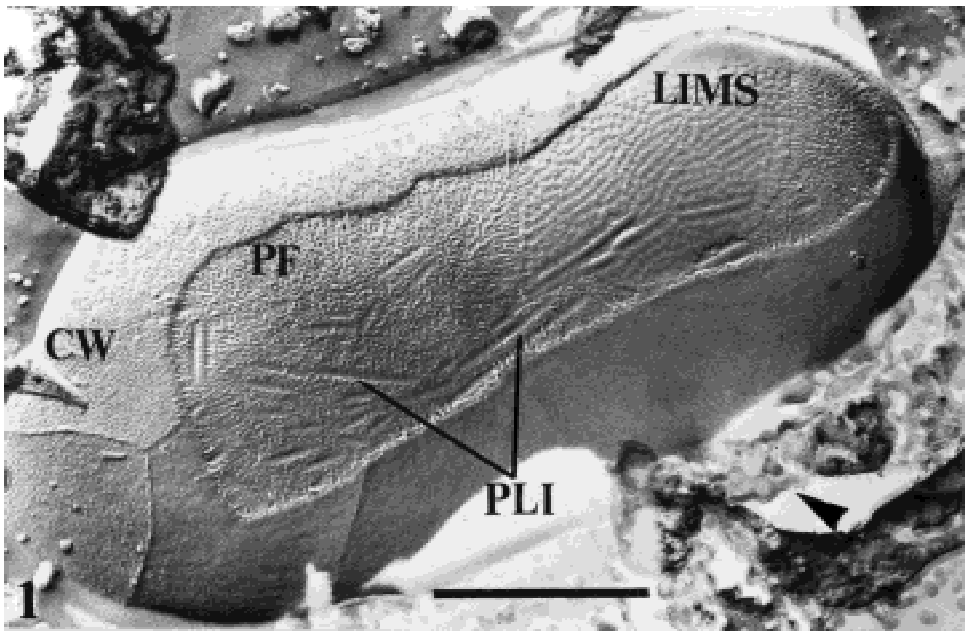
LIMS
PF
CW
PLI
1

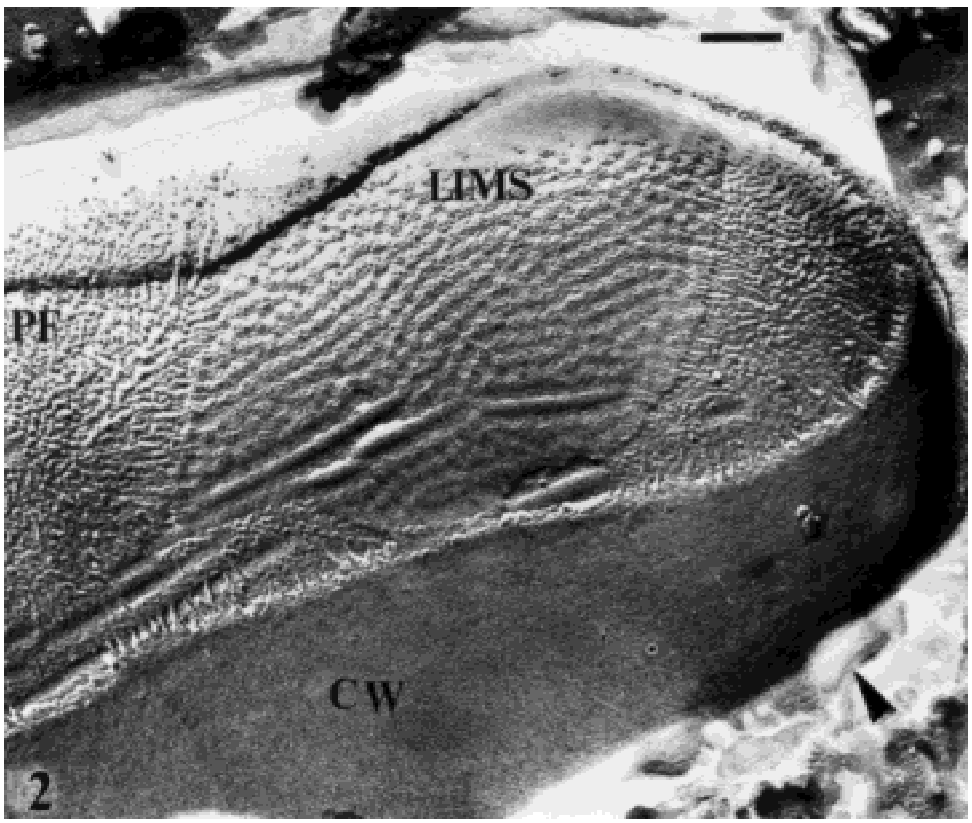
LIMS
PF
CW
2

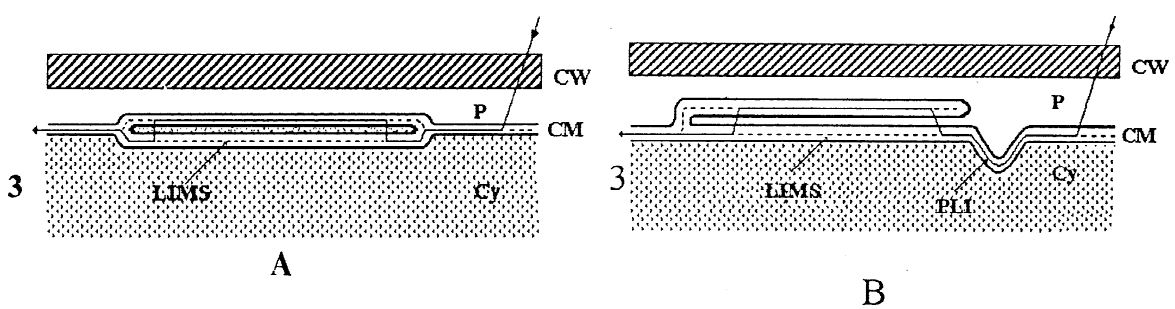
CW
P
CM
3
LIMS
Cy
A
CW
P
CM
3
LIMS
PLI
Cy
B

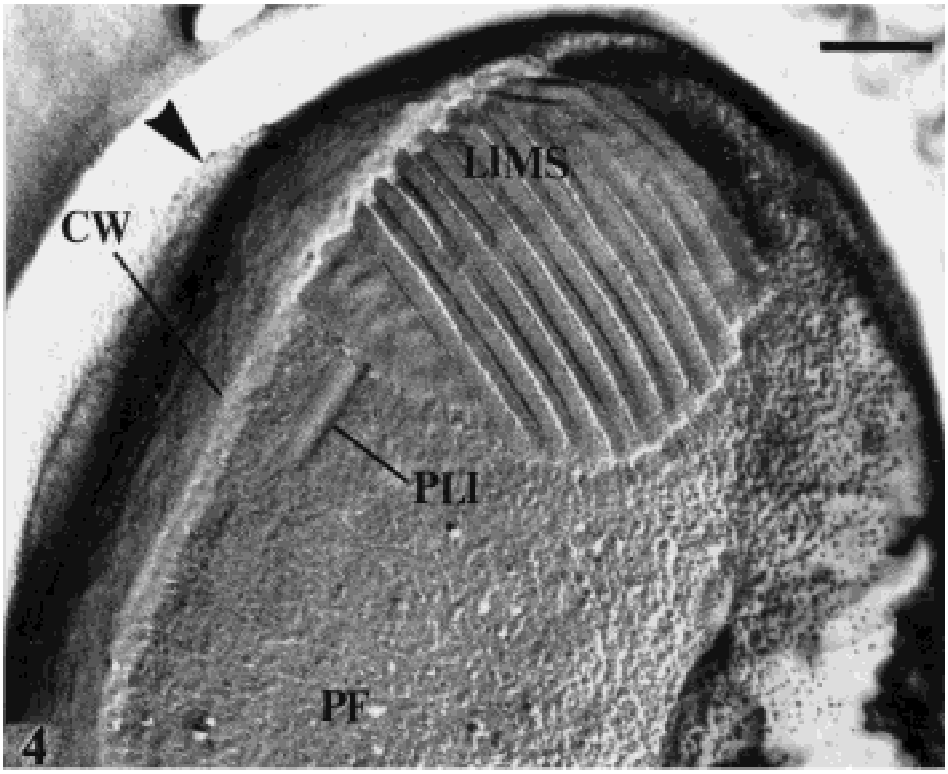

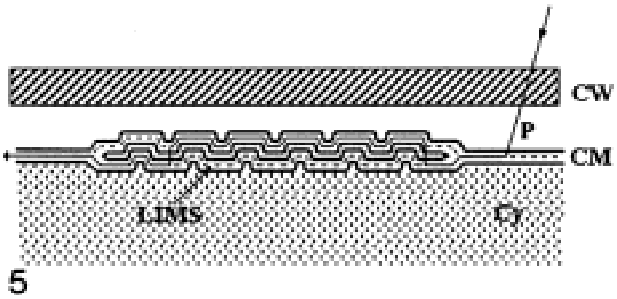

Figs. 1, 2, 4, and **6–9.** Electron micrographs of the freeze-fracture replicas of *Sulfobacillus thermosulfidooxidans* cells. Pocketlike invaginations of the CM are seen in Figs. 1, 2, 4, and 7. LIMSs are presented in Figs. 1, 2, 4, and 6–9. Figs. 1, 2, 4, 7, and 8 show the PF face of the CM, and Fig. 6 shows its EF face. Figure 9 presents the replica of a freeze-fractured spore-bearing cell with the PF face of the inner sporal membrane containing ridged LIMS. CM, cytoplasmic membrane; SR, smooth region; PF and EF, the PF and EF faces of the freeze-fractured CM; CW, cell wall; S, the S layer of the envelope; IMP, intramembrane particle; LIMS, lamellar intramembrane structure; PLI, the pocket-like invagination of CM; E, endospore; Cy, cytoplasm; P, periplasm; and Sph, spherical particles. Large dark arrowhead shows the direction of shadowing. Figures 1 and 6–9, bar = 0.5 μm; Figs. 2 and 4, bar = 0.1 μm. **Figs. 3, 5.** Drawing illustrating the electron microscopic image of the LIMS shown in Fig. 2 and 4, respectively, the most likely direction of fracture, and the formation of PF face. (*A*) closed inverted membrane; (*B*) open inverted membrane. For designations, see the legend to Figs. 1–9.

CMs may contain a number of digitate outgrowths whose cross sections have a trilaminar appearance. This implies that these outgrowths are formed by the invagination of only the outer layer of the CM, since, if the outgrowths were formed by the invagination or folds of lipid bilayer, their cross sections would have a pentalaminar appearance and the central lamina would represent a thick electron-dense layer composed of two hydrophilic sublayers. Therefore, the variant depicted in Fig. 16 is excluded. The distal parts of periplasmic evaginations merged with the CM lipid bilayer, as indicated by arrows in Figs. 14 and 19, to form lamellar inverted membrane structures (LIMSs). If one membrane locus contain several evaginations, this gives rise to multilayer LIMS. Generally, the percentage of cells with LIMSs reached 18–20 (*see* Table). Some difference with the data obtained from the freeze-fracture method can be explained by the fact that this method examines large membrane areas, while the thin sectioning reveals only small part of CMs. It should also be taken into account

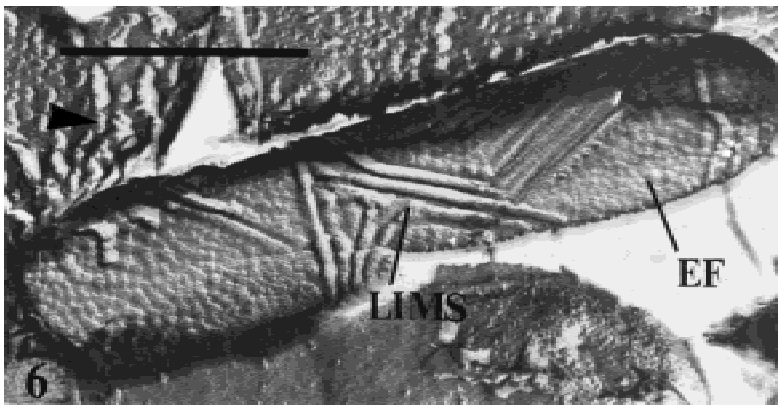

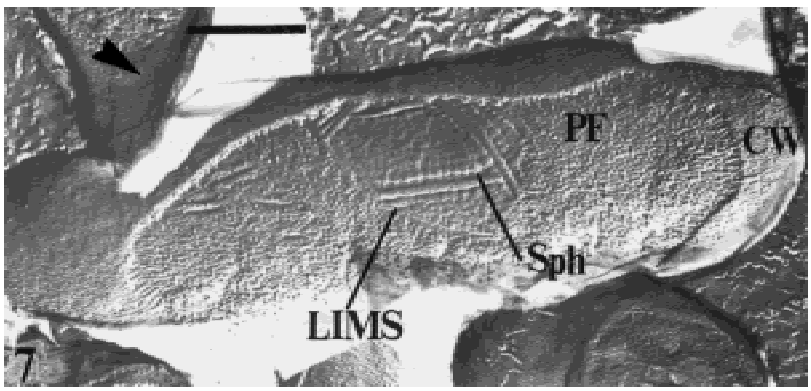

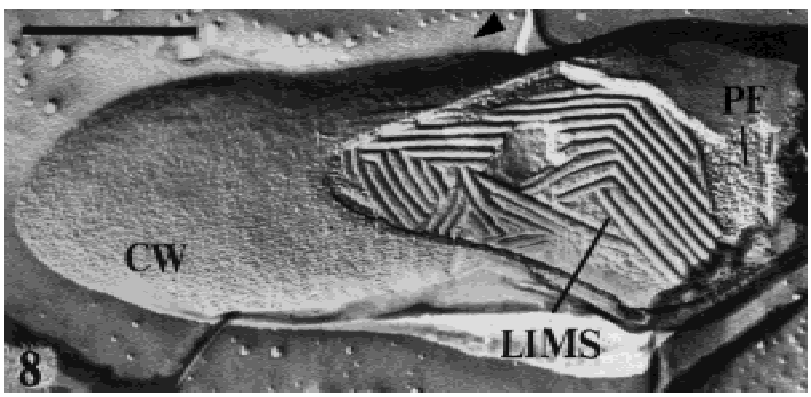

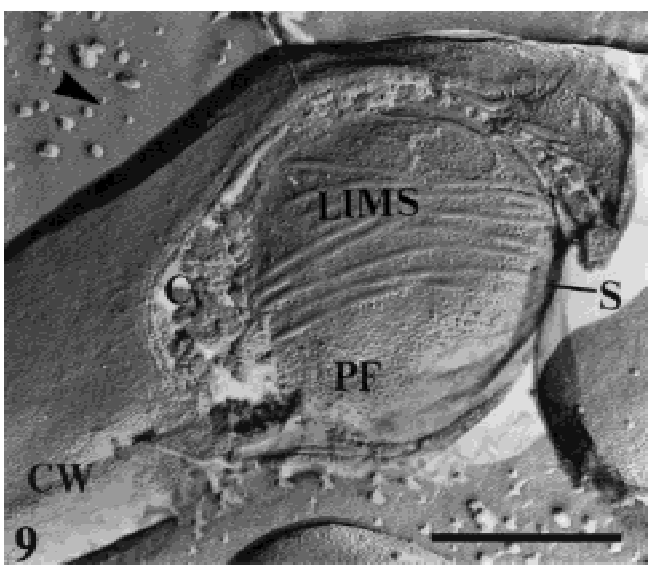

Figs. 6–9.

that, unlike the freeze-fracture method, the thin sectioning may lead to a number of artifacts.

As can be seen from the cell cross section given in Fig. 14, the length of the LIMS leaflets is about ⅓ of the length of the CM, which agrees with the data on the size of the LIMS leaflets observed on freeze-fracture replicas. Figures 14 and 19 show that the electron-transparent outer layer of a trilaminar leaflet is about 20 Å thicker than the analogous layer of the inner leaflets of LIMS and CM. These data, together with observed changes in the IMP composition, evidence that the formation of LIMSs is accompanied by a modification of membranes.

Similar LIMSs were also observed in cells of the other bacterium studied, *An. polyendosporus.* Moreover, analysis of the freeze-fractured cells of this bacterium allowed some new features of the structural organization of LIMS to be obtained. Replicas of freeze-fractured *An. polyendosporus* cells exhibited the presence of the convex inner leaflet (PF face) and the concave outer leaflet (EF face) of the cytoplasmic membrane (Figs. 22–31). The PF face contained a great number of intramembrane particles (IMPs) 9 to 12 nm in size, whereas the number of such particles on the EF face was considerably less, which is also typical of membranes of other bacterial species (Murray, 1978; Vaisman, 1981; Mayer, 1999). The distribution of IMPs over the faces was not uniform: there were numerous smooth zones on these faces, often having the form of round (Fig. 23) or polygonal plaques and strips (Figs. 22, 24, 26, 28, 30). In many instances, these zones had two or more layers. Correspondingly, the replicas of freeze-fractured membranes exhibited not only the PF (Fig. 22, 24, 28) or EF face (Fig. 26, 30) but also other layers overlying the faces. Such a location of these layers on replicas suggest that in situ they are located in the hydrophobic interior between the outer and inner leaflets of the CM. The intramembrane structures (IMSs) discussed, which were named flat lamellar intramembrane structures (LIMSs), may consist of one or a few layers, so that their freeze-fracture replicas have one layer about 50 Å in thickness (Figs. 24 and 26) or several such layers. For instance, the freeze-fracture replica of the LIMS shown in Fig. 30 had three layers overlying the EF face, which were evidently formed as a result of shifting the fracture plane from one membrane leaflet to another. As can be seen from Figs. 28 and 30, which show multilayer LIMSs, LIMS leaflets can lie below the fracture plane of the PF and EF faces. The uneven edges of the LIMS leaflets are probably due to the different adhesion of different layers of LIMS. Generally, LIMSs can be observed on both faces of the plasma membrane (Figs. 24–31) and may be 20-to-30 nm wide and 2-to-3 μm long. Unlike the PF face and EF face of the cytoplasmic membrane, LIMSs lacked IMPs of usual sizes but had sparse IMPs of larger sizes (about 150 nm in diameter) (Figs. 22 and 24), which presumably represented lipid particles. At the same time, the LIMS layers adjacent to the outer layer of the CM generally did not contain large IMPs (Figs. 26 and 30). In *An. polyendosporus* cells grown on potato agar or in synthetic medium, LIMSs could be observed in different growth phases. The predominant location of LIMSs was subcentral, although they might occur in different parts of the cell. Extended, sometimes multilamellar, LIMSs were most frequent in the cells of cultures grown as lawns on solid media and kept aerobically at +5°C during a period from several hours to three days. Analysis of the freeze-fractured cells of *Clostridium acetobutylicum*, *Alicyclobacillus acidocaldarius*, and *Saccharomyces cerevisiae* showed the presence of membrane structures similar to the LIMS of the two bacteria described above. However, the percentage of LIMS-containing cells in this case was low (V.I. Duda, T.S. Kalebina and N.E. Suzina, *in preparation*).

Discussion

The possible existence of inverted lamellar lipid membranes was first shown in experiments with artificial membranes (Cullis et al., 1980; Quin & Williams, 1983). In this paper, we present electron microscopic evidence that LIMSs are formed in the membranes of bacterial cells grown in optimal nutrient media at normal growth temperatures and pH values. The evidence was obtained from the analysis of freeze-fracture replicas and thin sections prepared by conventional methods of fixation and embedding and by the freeze-substitution technique. The location of LIMSs in the hydrophobic interior of the CM follows from the occurrence of these structures on both PF and EF faces of freeze-fracture replicas and from the specific appearance of LIMSs on thin sections, where they look like inverted lipid membranes bounded by the CM monolayer leaflets. Analysis of the structural organization of LIMSs showed that they may be multilamellar with smooth leaflets of different length and exterior; they distinctly differ from the common IMPs of the CM; paired membranes may have the form of thylakoids; in cross thin sections, the peripheral regions of the CM are bifurcate; in sulfobacilli, LIMSs have a corrugated appearance (Figs. 4, 8, 9 and diagram *C* Fig. 32). LIMSs can be formed either by the invagination of the outer leaflet of the CM (*see* Figs. 15, 19 and scheme *B* in Fig. 32) or by the fusion of intramembrane lipid vesicles, as follows from the analysis of electron micrographs in Figs. 7 and 32*E*. The mechanism of LIMS formation through the fusion of inverted lipid vesicles has also been postulated for artificial lipid membranes (Cullis et al., 1980; Quinn & Williams, 1983), although the latter substantially differ from natural biomembranes in chemical composition and physicochem-

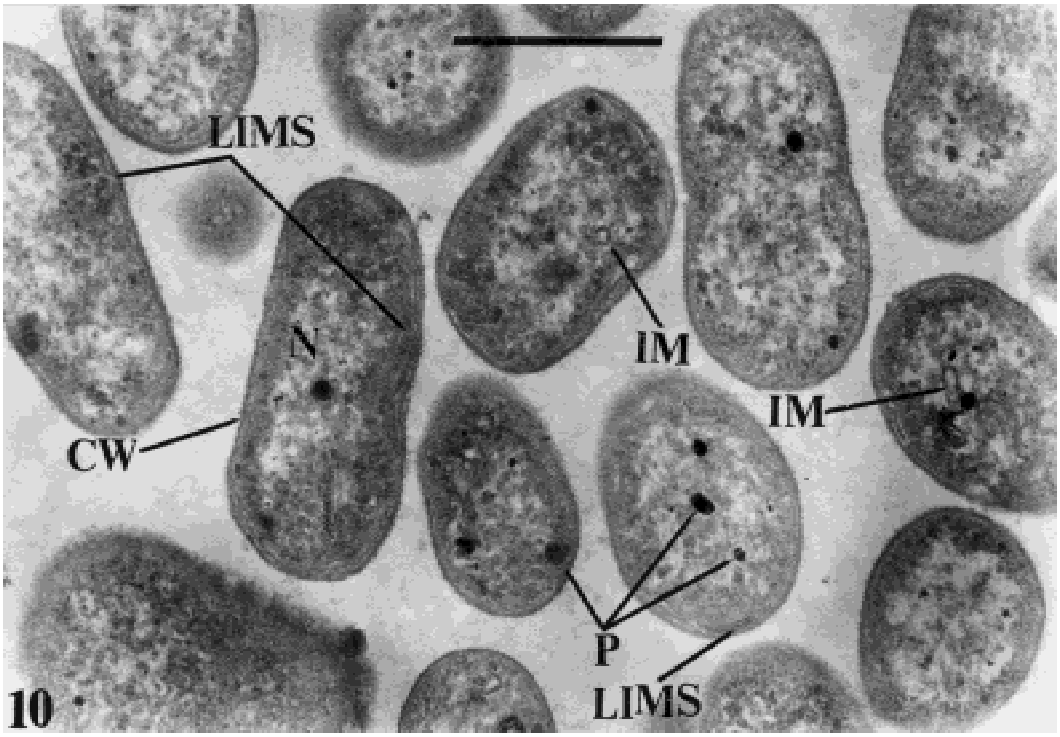

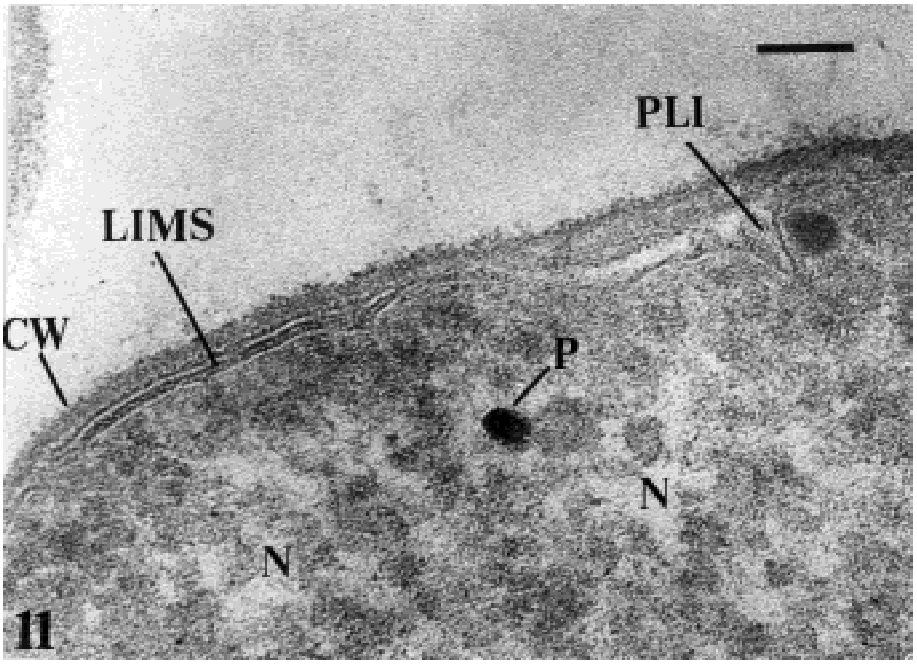

Fig. 10. General view of cells with LIMSs. Bar = 1.0 μm. Figs. 10–21. Electron micrographs of the ultrathin sections of *Sulfobacillus thermosulfidooxidans* cells. IM, intracytoplasmic membrane stricture; E, the CM evagination; N, nucleoid; P, polyphosphate granules. For other designations, *see* the legend to Figs. 1–9. **Figs. 11** and **12.** Fragments of the thin sections of *S. thermosulfidooxidans* cells with one unit LIMS. Bar = 0.1 μm. **Fig. 13.** Drawing illustrating the structure of the LIMSs shown in Figs. 11 and 12. **Fig. 14.** Unit LIMS with the lateral region of the periplasmic evaginate of the outer lipid layer (arrow) which is not fused with the CM. The cross section of the evaginate has two outer electron-dense layer and central electron-opaque layer. Double arrow points to the exit of the evaginate from the CM and its distal region. Bar = 0.1 μm. **Fig. 15.** Drawing illustrating the structure of the LIMSs shown in Fig. 14. **Fig. 16.** Drawing of the trilaminar periplasmic evaginate (fold) of the CM, whose cross section has six layers.

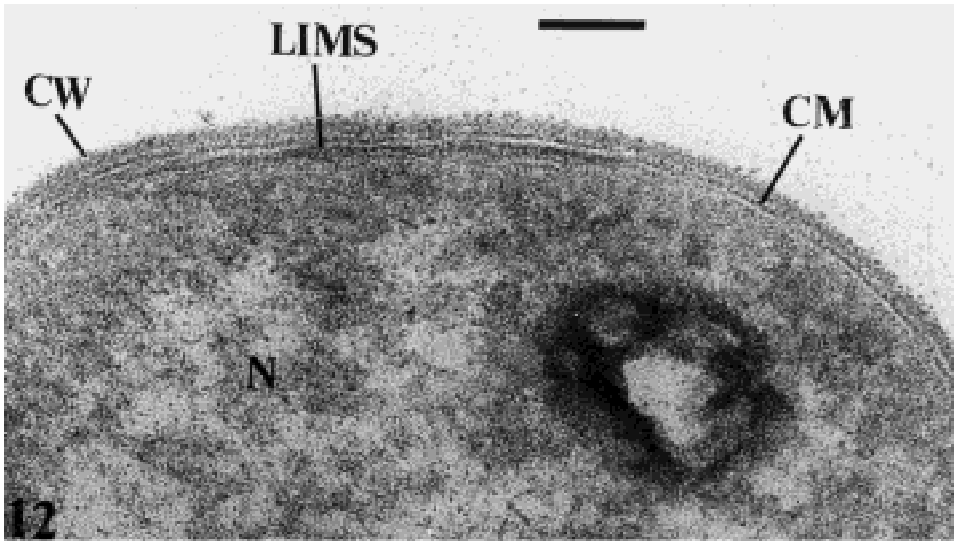
LIMS
CW
CM
N
12

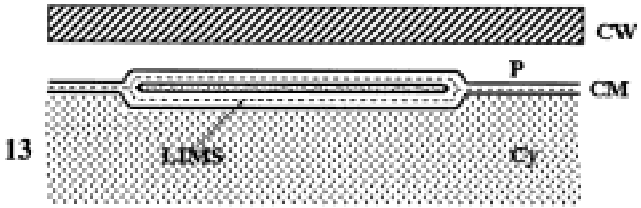
CW
P
CM
13
LIMS
Cy

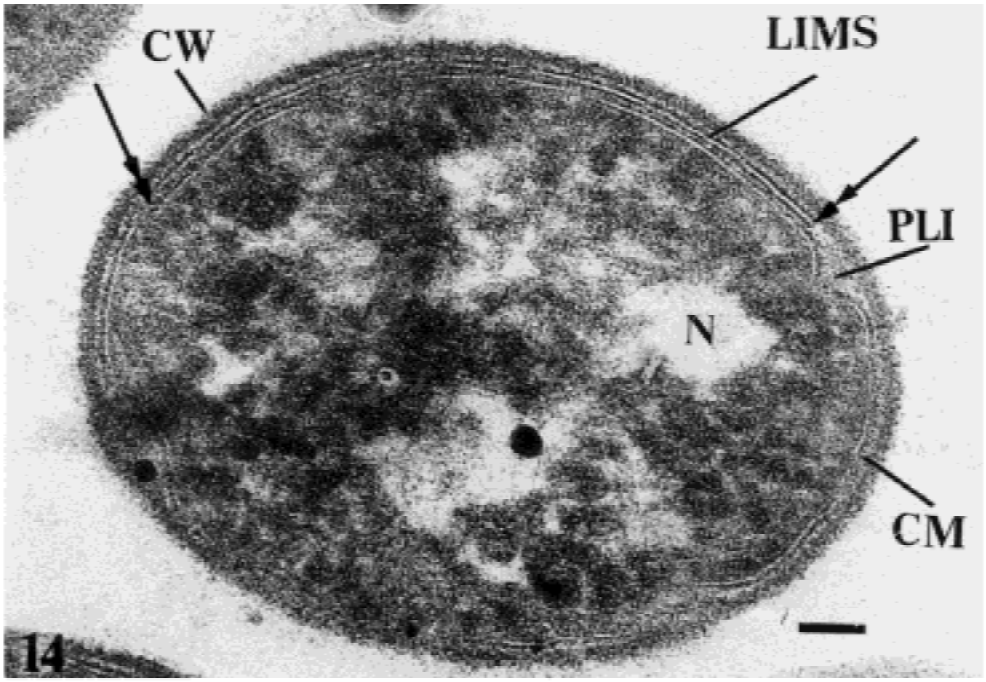
CW
LIMS
PLI
N
CM
14

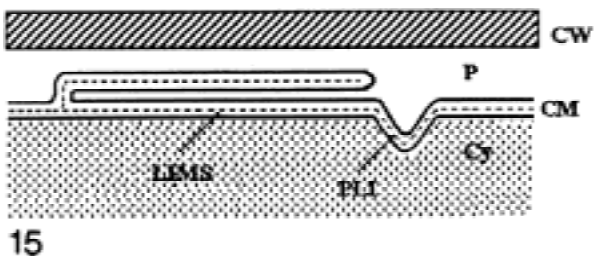
CW
P
CM
LIMS
PLI
Cy
15

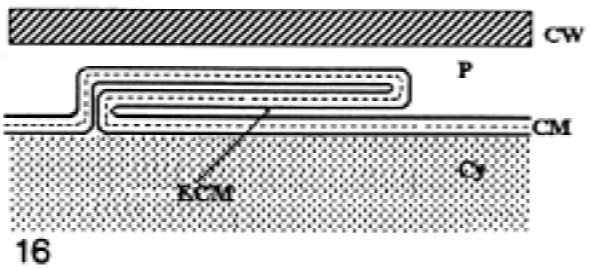
CW
P
CM
ECM
Cy
16

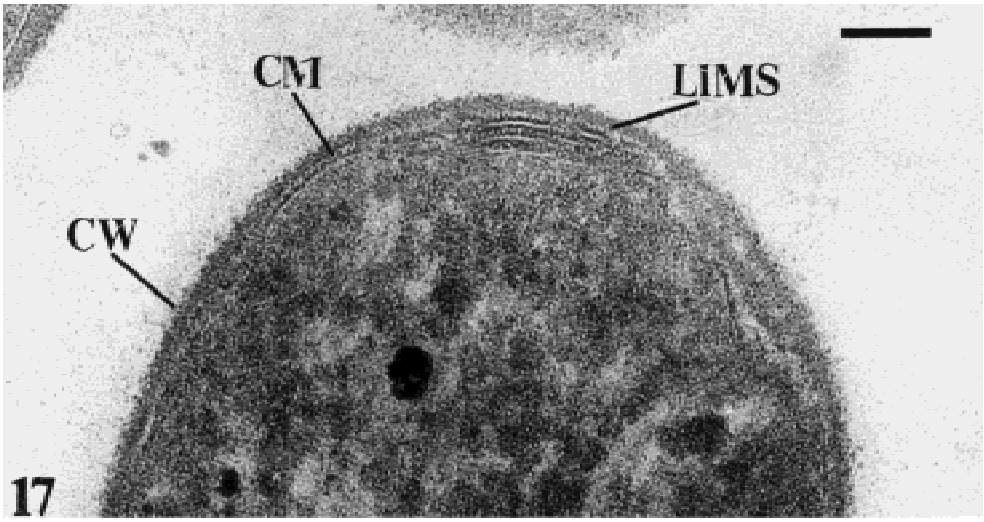

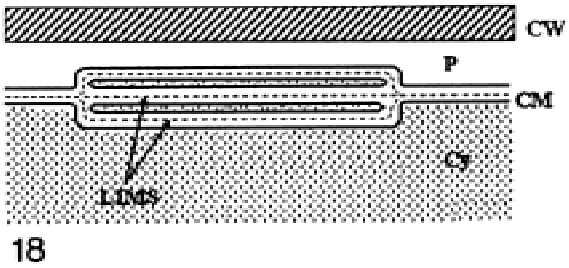

Fig. 17. Electron micrograph of the CM region with two unit LIMSs. Bar = 0.1 μm. **Fig. 18.** Drawing illustrating the structure of the LIMSs shown in Fig. 17. **Fig. 19.** Multilamellar LIMS. Bar = 0.1 μm. **Fig. 20.** Drawing illustrating the likely structure of the multilamellar LIMS shown in Fig. 19. **Fig. 21.** Freeze-substitution thin section with LIMSs. Bar = 0.1 μm.

ical properties. The formation of lipid vesicles inside the lipid bilayer of membranes may occur through the fusion of the CM near growing septa in the process of cell division and probably through the local accumulation of newly synthesized lipids in some regions of the CM.

The evagination of the outer leaflet of the CM toward the periplasm may be due to a differential distribution of intramembrane lateral pressure, which depends on the composition of the lipid bilayer (Cantor, 1999). The outer leaflet of the CM seems to evaginate more easily than its inner leaflet, since the latter contains more IMPs and is bound to ribosomes, nucleoplasm, and the bacterial cytoskeleton, which resembles that of eukaryotes (Margolin, 1998). The lipid asymmetry of bacterial membranes should also be taken into account (Op den Kamp, 1979; Devaux, 1991). The evagination of the outer layer of the CM is of interest in relation to the biogenesis of the outer membrane of the cell wall (or second lipoprotein membrane) of gram-negative bacteria. In particular, the vegetative cells of the recently isolated spore-forming bacteria *Sporomusa* (Moller et al., 1984) and *Sporohalobacter* (Oren & Stackebrandt, 1987) possess such membrane. As spores are known to have no CW, outer membrane must rapidly form during spore outgrowth. In this case, it would be reasonable to suggest that the outer membrane of the CW is formed through the evagination and expansion of the outer leaflet of the sporal CM.

The reason for the corrugated appearance of *S. thermosulfidooxidans* LIMSs and the presence of PLIs in the membranes of this bacterium still remains unknown; however, we may relate this to the specific lipid composition of membranes of this organism. Indeed, as shown by Tsaplina et al. (1994), the membrane lipids of *S. thermosulfidooxidans* VKM B-1269 contain from 30 to 60–70% ω-cyclohexanoic acid, depending on the growth conditions. At the same time, the fatty acid composition of *An. polyendosporus* membranes is different and resembles that of butyric acid clostridia, whose major fatty acids are myristic (C14:0), palmitic (C16:0), and hexadeconic (C16:1) acids (V.I. Duda et al., *submitted*). Thus, the characteristic constituents of membranes of clostridia and *An. polyendosporus* are plasmalogens, whose actual effect on the structure and function of LIMSs is to be elucidated.

The general functions of LIMSs are probably the

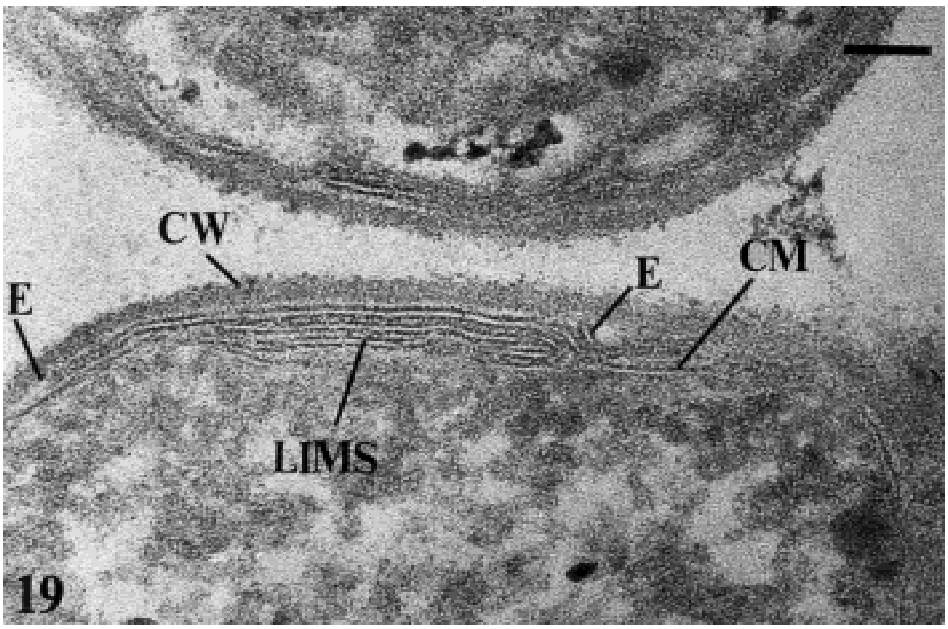

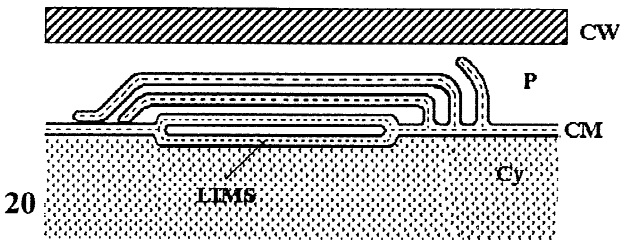

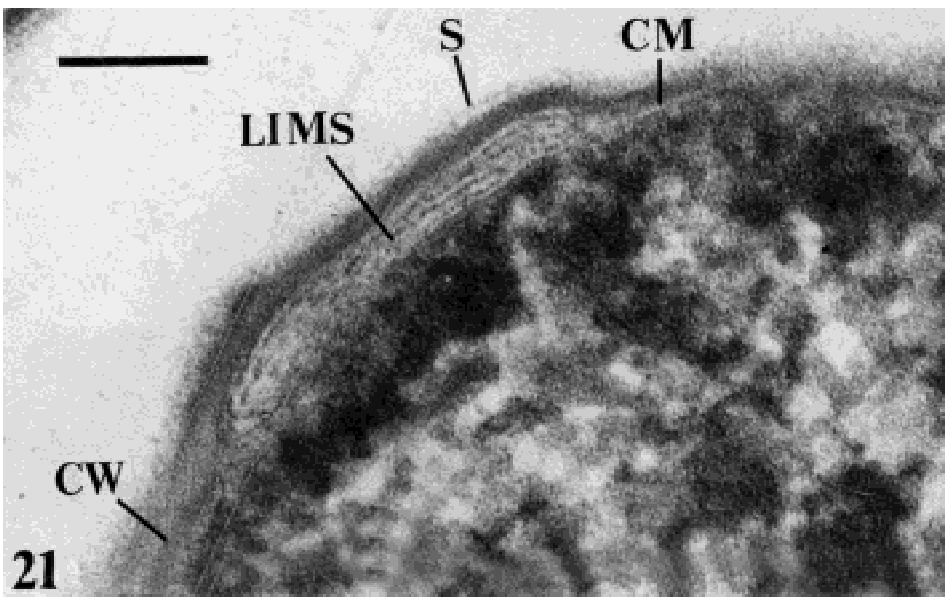

same as those of the nonbilayer regions of biomembranes (Cullis et al., 1980; Verkleij, 1984; Norris, 1989; Duong et al., 1997). We believe that LIMSs may represent a reserve of lipids and membrane units, which are utilized during the active growth of cells or when it is necessary to rapidly enlarge the reserve of membranes, to repair them, to form intracytoplasmic membrane structures of the mesosome type, or to relieve membrane tension. Alternatively, LIMSs may be involved in the translocation of lipids across the membrane and in the processes related to cell growth and differentiation, such as the separation of nucleoids, formation of septa, and sporogenesis.

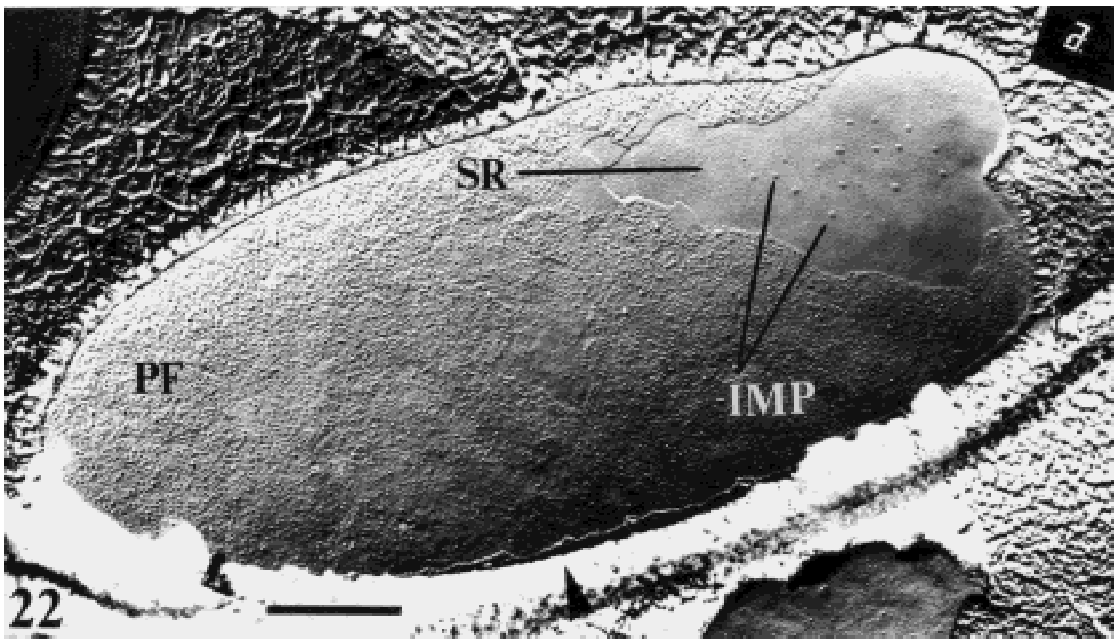

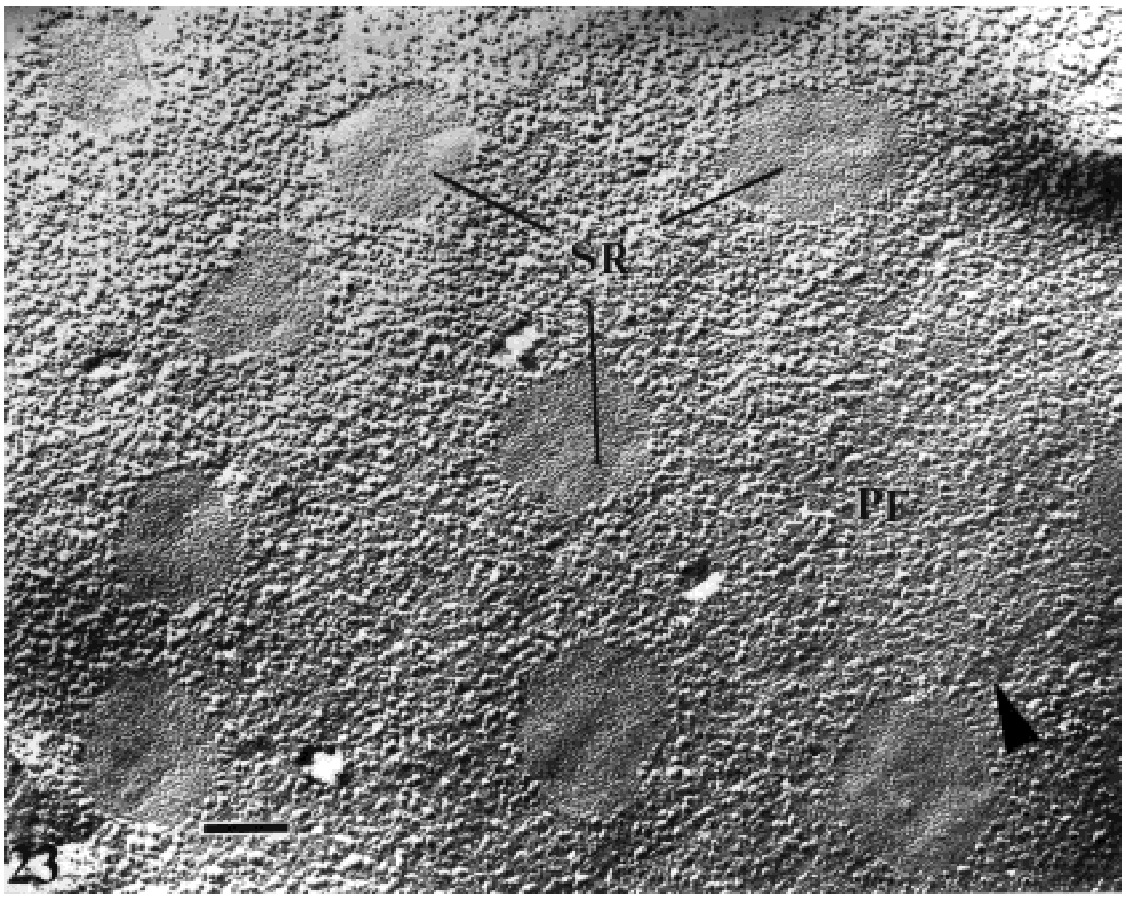

Fig. 22. PF face of the CM containing an extended smooth polar region with scarce large IMPs. Bar = 0.5 μm. Figs. 22–29. Electron micrographs of freeze-fracture replicas of *Anaerobacter polyendosporus* strain PS-1 cells grown on potato agar (Figs. 22–24, 26, 28, 30) and kept aerobically at +5C for 24 hr (Fig. 29). **Fig. 23.** PF face of the CM with the round smooth regions lacking IMPs. Bar = 0.1 μm. **Fig. 24.** PF face of the CM containing an extended region of LIMS with large IMPs. Bar = 0.1 μm. **Fig. 25.** Drawing illustrating the membrane structure shown in Fig. 24. **Fig. 26.** EF face of the CM containing an extended region of LIMS with scarce IMPs. Bar = 0.1 μm. **Fig. 27.** Drawing illustrating the fracture of the CM and the formation of the EF face shown in Fig. 26.

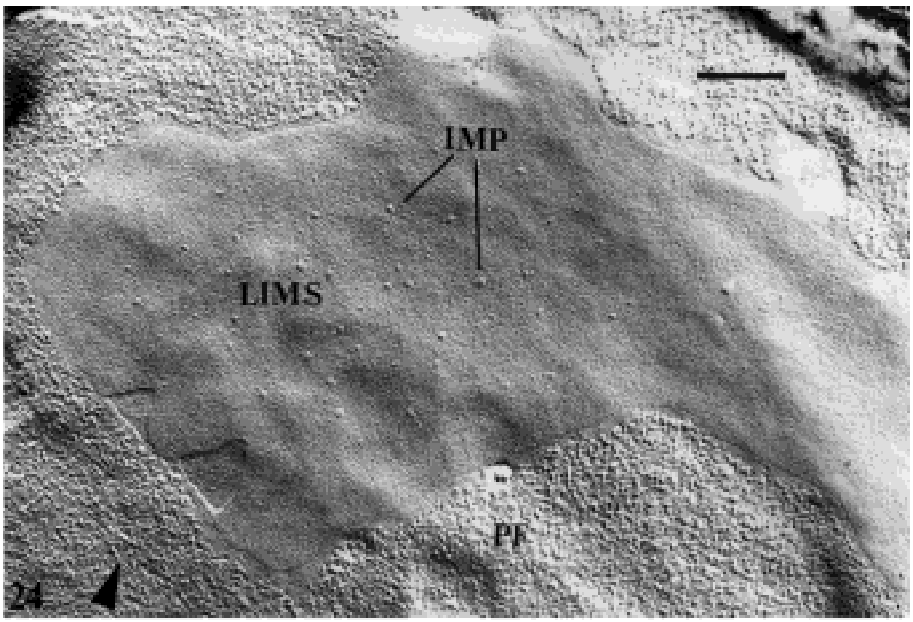

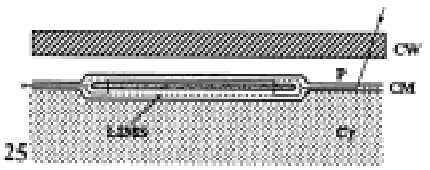

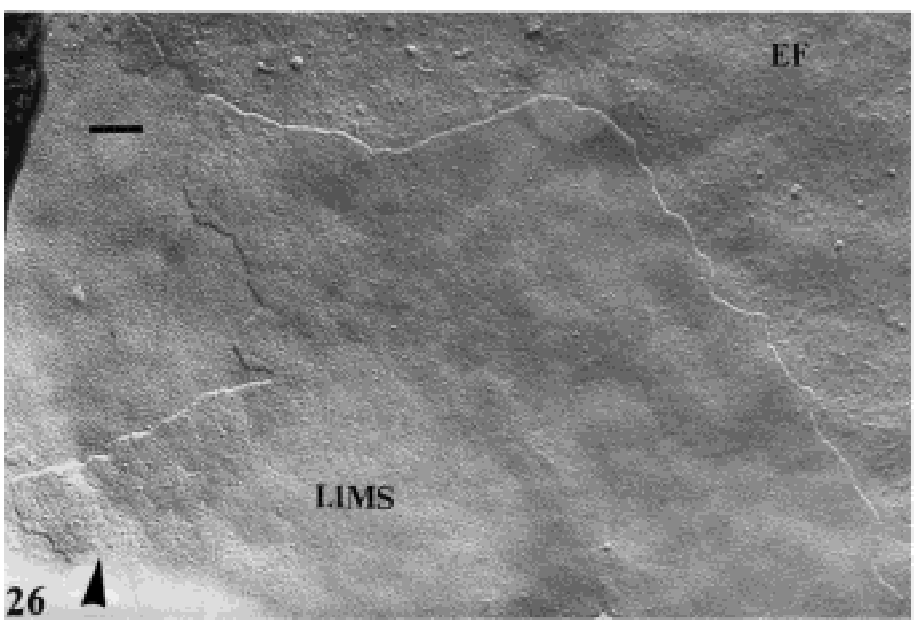

Some functions of LIMSs may be species-specific. In sulfobacilli, these structures are most likely involved in the oxidation of sulfur. In view of this, of interest is the recent suggestion about the involvement of discrete multilamellar membrane structures in sulfur transport in sulfide-oxidizing bacteria (Taylor & Wirsen, 1997).

LIMSs may be responsible for the tolerance of the

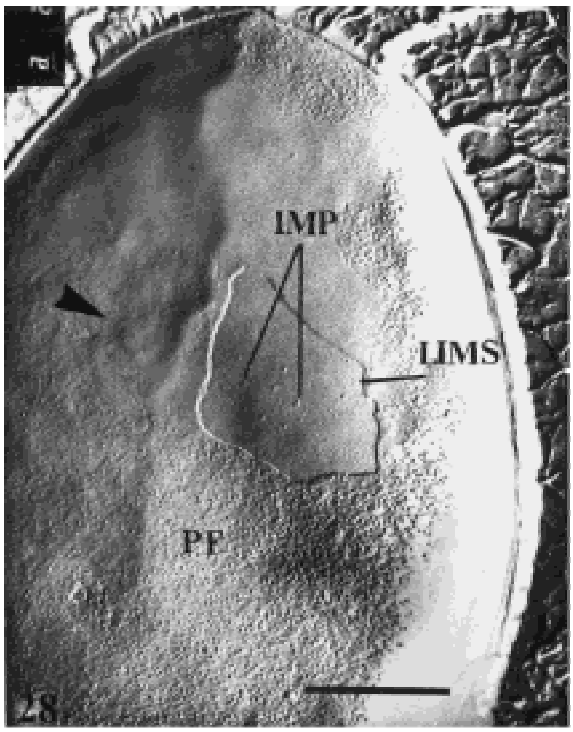

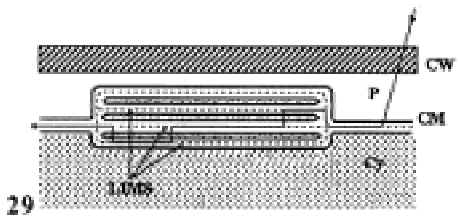

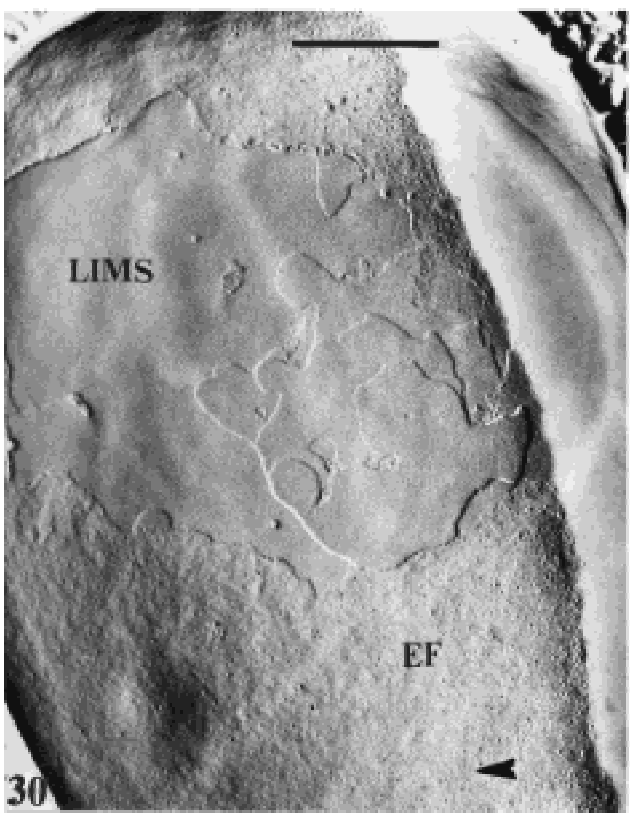

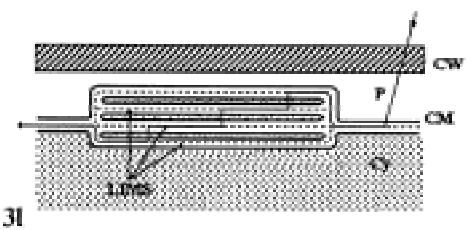

Fig. 28. PF face of the CM with a region of multilamellar LIMS. Bar = 0.5 μm. **Fig. 29.** Drawing illustrating the fracture of the CM and the formation of PF face with LIMS in the CM layer adjacent to the cytoplasm (*see* Fig. 28). **Fig. 30.** EF face of the CM with a region of multilamellar LIMSs. Bar = 0.5 μm. **Fig. 31.** Drawing illustrating the formation of the EF face and multilamellar LIMS shown in Fig. 30. Due to different mutual adhesion of different regions of the LIMS layers, the fracture plane can shift from one membrane leaflet to another. EF face is formed by the upper CM layer adjacent to the CW.

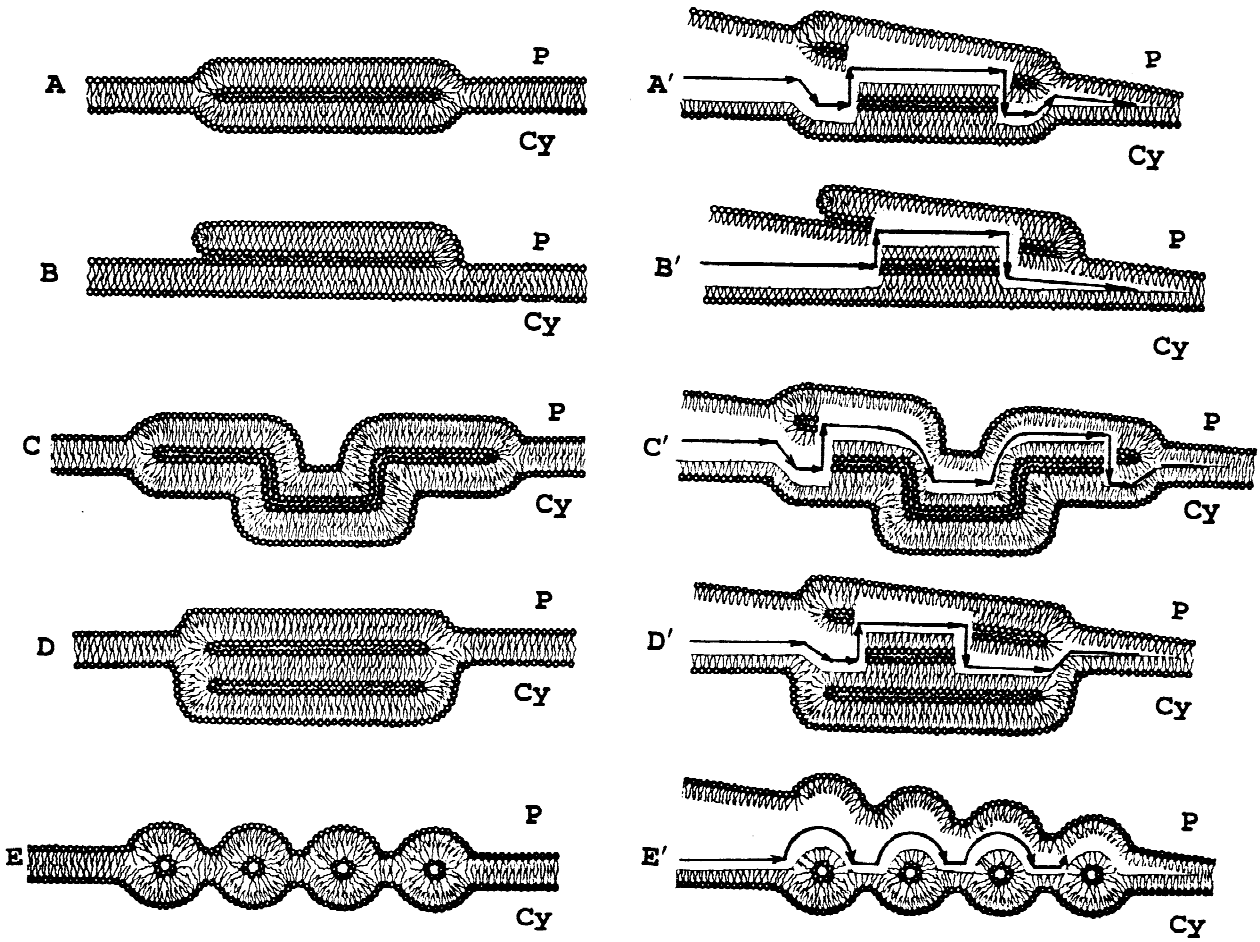

Fig. 32. Schematic representation of the arrangement of lipid molecules in the CM and LIMS deduced from the results of electron microscopic studies. *A* and *D* represent flattened LIMSs with the smooth surface, either pentalamellar (*A*) or heptalamellar (four electron-dense and three electron-transparent layers (*D*); *B* is an evagination of the outer leaflet of the CM toward the periplasmic space; *C* shows LIMSs with a corrugated appearance; and *E* represents the rows of lipid vesicles in the hydrophobic interior of the CM. P and Cy stand for the periplasmic and cytoplasmic sides of the CM, respectively. A′, B′, C′, D′, and E′ show the likely directions of the fracture of CM, LIMS, and lipid vesicles.

obligately anaerobic bacterium *An. polyendosporus* to oxygen: the vegetative cells of this bacterium incubated on solid nutrient media in the presence of atmospheric oxygen remain viable during 3–7 days. After 1–3 days of such incubation, the number of LIMSs and their mean size in *An. polyendosporus* cells considerably increased (Fig. 30). As for the effect of the lipid composition of membranes on their permeability to oxygen, it has been demonstrated by Subczynki, Hyde and Kusumi, 1989. In cyanobacteria, surface structures formed by heterocysts considerably decrease the penetration of oxygen into cells (Walsby, 1985). The functional role of LIMSs in microorganisms is to be elucidated in depth.

LIMSs and intramembrane lipid vesicle are specific compartments within the lipid bilayer of the CM, whose existence is indicative of complex compartmentalization processes in biomembranes. The formation of similar membrane structures had been predicted by Cullis et al. (1980) in their study of artificial lipid membranes. The presence of LIMSs in such dissimilar microorganisms as anaerobic heterotrophic mesophilic bacteria and aerobic mixotrophic thermoacidophilic bacteria suggests that they may be common to many microorganisms.

This work was supported by grants 99-04-49144, 99-04-49145, and 99-04-49146 from the Russian Foundation for Basic Research.

References

Borovjagin, V.L., Sabelnikov, A.G. 1989. Lipid polymorphism of model and cellular membranes are revealed by electron microscopy. *Electron Microscopy Rev.* **2:**75–115

Borovijagin, V.L., Sabelnikov, A.G., Tarahovsky, Y.S., Vasilenko, J.A. 1987. Polymorphic behavior of Gram-negative bacteria membranes. *J. Membrane Biol.* **100:**229–242

Borovjagin, V.L., Vergara, J.A., McIntosh, T.J. 1982. Morphology of

the intermediate stages in the lamellar to hexagonal lipid phase transition. *J. Membrane Biol.* **69:**199–212

Cantor, R.S. 1999. Lipid composition and the lateral pressure profile in bilayers. *Biophys. J.* **76:**2625–2639

Cullis, P.R., De Kruijff, B., Hope, M.J., Nayar, R., Schmidt, S.L. 1980. Phospholipids and membrane transport. *Can. J. Biochem.* **58:**1091–1100

Devaux, P.F. 1991. Static and dynamic lipid asymmetry in cell membranes. *Biochemistry.* **30:**1163–1173

Duda, V.I., Lebedinsky, A.V., Mushegjan, M.S., Mitjushina, L.L. 1987. A new anaerobic bacterium forming up to five endospores per cell, *Anaerobacter polyendosporus* gen. et spec. nov. *Arch. Microbiol.* **148:**121–127

Duong, F., Eichler, J., Price, A., Leonard, M.R., Wickner, W. 1997. Biogenesis of the Gram-negative bacterial envelope. *Cell* **91:**567–573

Epand, R.M. 1998. Lipid polymorphism and protein-lipid interaction. *BBA Rev. Biomembranes* **1376:**353–368

Fikhte, B.A., Zaichkin, E.I., Ratner, E.N. 1973. New methods of specimen preparation for electron microscopy of biological objects. Moscow. Nauka. (*in Russian*)

Gliozzi, A., Rolandi, R., De Rosa, M., Gambacorta, A., Nicolaus, B. 1982. Membrane models of *Archaebacteria. In:* Transport in Membranes. Model Systems and Reconstitution. R Antohni et al., editors. Raven Press, New York

Golovacheva, R.S., Karavaiko, G.I. 1978. *Sulfobacillus*, a new genus of thermophilic spore-forming bacteria. *Mikrobiologiya.* **47:**815–822 (*in Russian*)

Hartree, J.F. 1972. Determination of protein: a modification of the Lowry method that give a linear photometric response. *Anal. Biochem.* **48:**422–427

Hoch, H.C. 1996. Freeze-substitution of fungi. *In:* Ultrastructure techniques for microorganisms. H.C. Aldrich and W.J. Todd, editors. pp. 183–212. Plenum Press, New York

Langworthy, T.A., Tornabene, T.G., Holzer, G. 1981. Lipids of *Archaebacteria. Zbl. Bakt. Hyg., I Abt. Orig.* **C3:**228–244

May, S., Ben-Shaul, A. 1999. Molecular theory of lipid-protein interaction and L_{α}-H_{II} transition. *Biophys. J.* **76:**751–767

Margolin, W. 1998. A green light for the bacterial cytoskeleton. *Trends in Microbiology.* **6:**233–238

Mayer, F. 1999. Cellular and subcellular organization of prokaryotes. *In:* Biology of the Prokaryotes. Part I Blackwell-Science. pp. 20–46. Thieme, Stuttgart, New York

Moller, B., Obmer, R., Howard, B.H., Cottschalk, G., Hippe, H. 1984. *Sporomusa*, a new genus of gram-negative anaerobic bacteria including *Sporomusa sphaeroides* sp. nov. and *Sporomusa ovata* sp. nov. *Arch. Microbiol.* **139:**388–398

Murray, R.G.E. 1978. Form and function. I. Bacteria. *In:* Essays in Microbiology. J.R. Norris and M.H. Richmond, editors. J. Willoy and Sons, Chichester

Moore, H., Muhletaler, K. 1963. Fine structures in frozen-etched yeast cells. *J. Cell Biol.* **17:**609–628

Norris, V. 1989. Phospholipid flip-out controls the cell cycle of *Escherichia coli. J. Theor. Biol.* **139:**117–128

Op den Kamp, J.A.F. 1979. Lipid asymmetry in membranes. *Ann. Rev. Biochem.* **48:**47–71

Oren, A.P.H., Stackebrandt, E. 1987. Transfer of *Clostridium lortetii* to a new genus *Sporohalobacter* gen. nov. as *Sporohalobacter lortetii* comb. nov., and description of *Sporohalobacter marismortui* sp. nov. *Syst. Appl. Microbiol.* **9:**239–246

Quinn, P.G., Williams, W.P. 1983. The structural role of lipids in photosynthetic membranes. *Biochim. Biophys. Acta* **737:**223–266

Reynolds, E.S. 1963. The use of lead citrate at high pH as an electron-opaque in electron microscopy. *J. Cell Biol.* **17:**208–213

Rolandi, R., Schindler, H., DeRosa, M., Gambacorta, A. 1986. Monolayers of the ether lipids from archaebacteria. *Eur. Biophys. J.* **14:**19–27

Severina, L.O., Senyushkin, A.A., Suzina, N.E., Karavaiko, G.I. 1998. Ultrastructural organization of the cell wall surface layer in *Sulfobacillus thermosulfidooxidans. Mikrobiologiya.* **67:**762–766 (*in Russian*)

Siunov, A.V., Nikitin, D.V., Suzina, N.E., Dmitriev, V.V., Kuzmin, N.P., Duda, V.I. 1999. The phylogenetic status of *Anaerobacter polyendosporus,* an anaerobic polysporogenic bacterium. *Int. J. Syst. Bact.* **49:**1119–1124

Subczynki, W.K., Hyde, J.S., Kuzumi, A. 1989. Oxygen permeability of phosphatidylcholine-cholesterol membranes. *Proc. Natl. Acad. Sci. USA* **86:**4474–4478

Suzina, N.E., Severina, L.O., Senyushkin, A.A., Karavaiko, G.I., Duda, V.I. 1999. Ultrastructural organization of membrane system in *Sulfobacillus thermosulfidooxidans. Microbiologiya.* **68:**491–500 (*in Russian*)

Taylor, C.D., Wirsen, C.O. 1997. Microbiology and ecology of filamentous sulfur formation. *Science* **277:**1483–1485

Tourova, T.P., Poltoraus, A.B., Lebedeva, I.A., Tsaplina, I.A., Bogdanova, T.I., Karavaiko, G.I. 1994. 16S ribosomal RNA (rDNA) sequence analysis and phylogenetic position of *Sulfobacillus thermosulfidooxidans. System. Appl. Microbiol.* **17:**509–512

Tsaplina, I.A., Bogdanova, T.I., Sayakin, D.D., Karavaiko, G.I. 1991. The effect of organic compounds on the growth and pyrite oxidation by *Sulfobacillus thermosulfidooxidans*. *Mikrobiologiya.* **60:**34–40 (*in Russian*)

Tsaplina, I.A., Osipov, G.A., Bogdanova, T.I., Nedorezova, T.P., Karavaiko, G.I. 1994. Fatty acid composition of lipids in thermoacidophilic bacteria of the genus *Sulfobacillus. Mikrobiologiya.* **63:**821–830 (*in Russian*)

Vaisman, I.S. 1981. Considerations on the value of freeze-etching technique in studying the ultrastructure of some anaerobic bacteria. *Acta Histochemica. Suppl.* **Band XXIII:**241–247

Verkleij, A.L. 1984. Lipidic intramembranous particles. *Biochim. Biophys. Acta* **779:**43–63

Walsby, A.E. 1985. The permeability of heterocysts to the gases nitrogen and oxygen. *Proc. Roy. Soc. London* **226:**345–366